Latest Spectroscopy results from ATLAS

Brad Abbott

University of Oklahoma

For the ATLAS collaboration

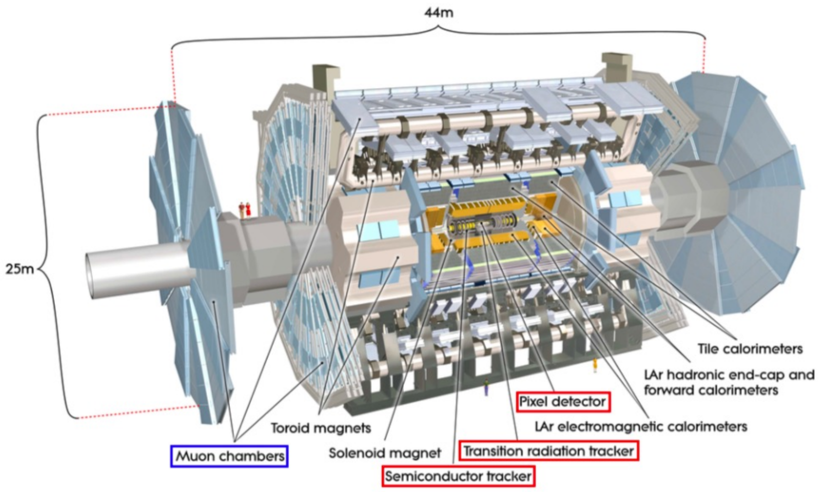

HQL 2021
University of Warwick
Sept 13-17, 2021

Outline

- Study of $J/\psi p$ resonances in the $\Lambda_b^0 \rightarrow J/\psi p K^-$ decays in *pp* collisions at 7 and 8 TeV with the ATLAS detector. (Pentaquark search)

  ATLAS-CONF-2019-048

- Study of the $B_c^+ \rightarrow J/\psi D_s^+$ and $B_c^+ \rightarrow J/\psi D_s^{*+}$ decays in pp collisions at $\sqrt{s}$= 13 TeV with the ATLAS detector. ATLAS-CONF-2021-046

- Search for a structure in $B_s^0\pi^\pm$ Invariant Mass spectrum with the ATLAS experiment. (X(5568) search) PRL 120, 202007 (2018)

- Relative B_c^+/B^+ production measurement at 8 TeV.

  Phys. Rev D 104, 012010 (2021)

Pentaquarks in $\Lambda_b^0 \to J/\psi p K^-$

History

LHCb

2 pentaquarks observed in $\Lambda_b^0 \to J/\psi p K^-$ (PRL 115,072001)
$P_c(4380)^+$ width ~205 MeV, $P_c(4450)^+$ width ~39 MeV

$\Lambda_b^0 \to J/\psi p \pi^-$ decays consistent with $\Lambda_b^0 \to J/\psi p K^-$ results (PRL 117,082003)

Larger data set of $\Lambda_b^0 \to J/\psi p K^-$
$P_c(4312)^+$, $P_c(4450)^+$ is two overlapping peaks $P_c(4440)^+$, $P_c(4457)^+$ (PRL 112,222001)

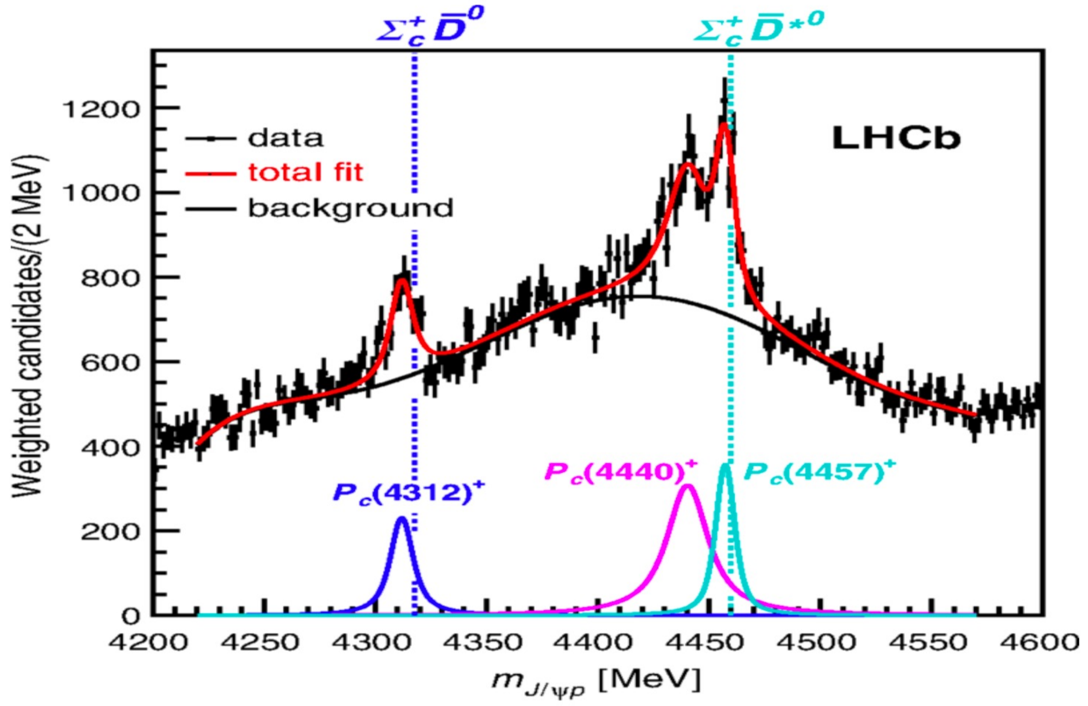

Not observed by GlueX Collaboration: PRL 123, 072001

D0 observed 3 σ evidence in J/ψ p events (arXiV:1910.11767)

Pentaquarks in $\Lambda_b^0 \to J/\psi p K^-$

No hadron identification in ATLAS so need to consider numerous states.

$J/\psi \to \mu^+\mu^-$
$p_T(\mu) > 4$ GeV ; $|\eta(\mu)| < 2.3$
$|m(J/\psi_{pdg}) - m(\mu^+\mu^-)| < 290$ MeV

B-hadron reconstruction
$|\eta(h_x)| < 2.5$
4-track vertex cuts on (μ^+, μ^-, h_1, h_2)
$p_T(H_b) > 12$ GeV, $|\eta(H_b)| < 2.1$
Mass, L_{xy} decay length and helicity cuts

$m(K\pi)$ and $m(\pi K) > 1.55$ GeV

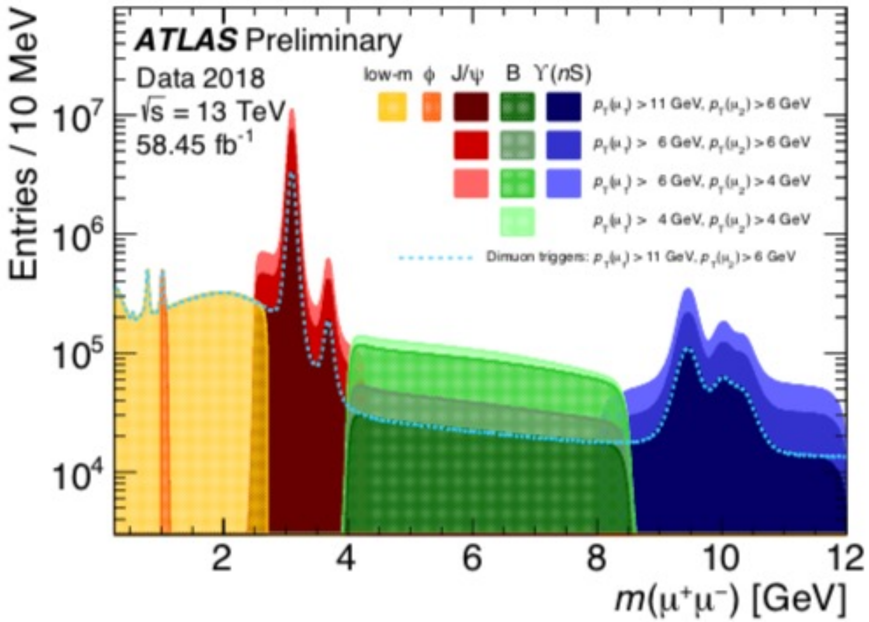

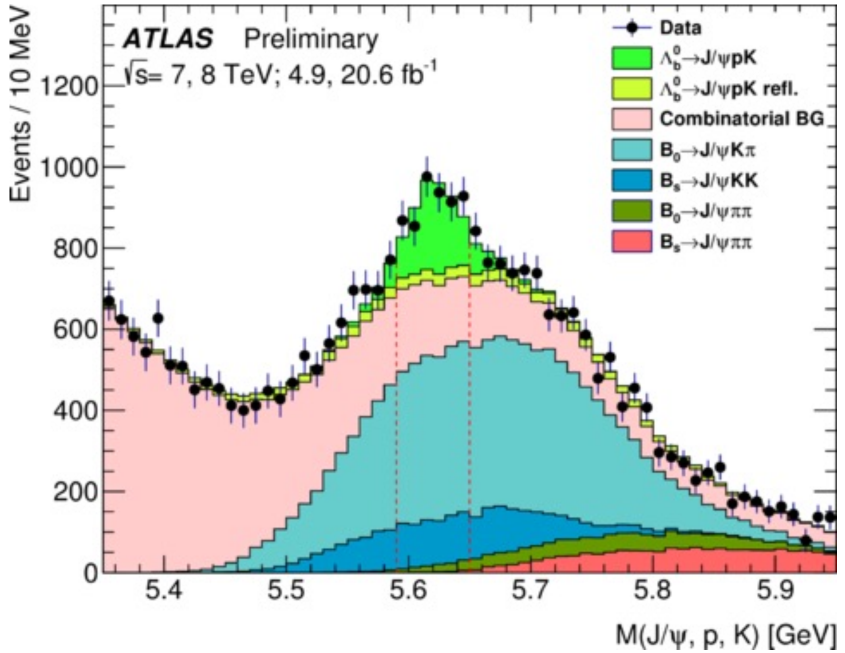

Pentaquarks in $\Lambda_b^0 \to J/\psi p K^-$

m(J/ψ p)

χ^2/N_{dof}=37.1/39

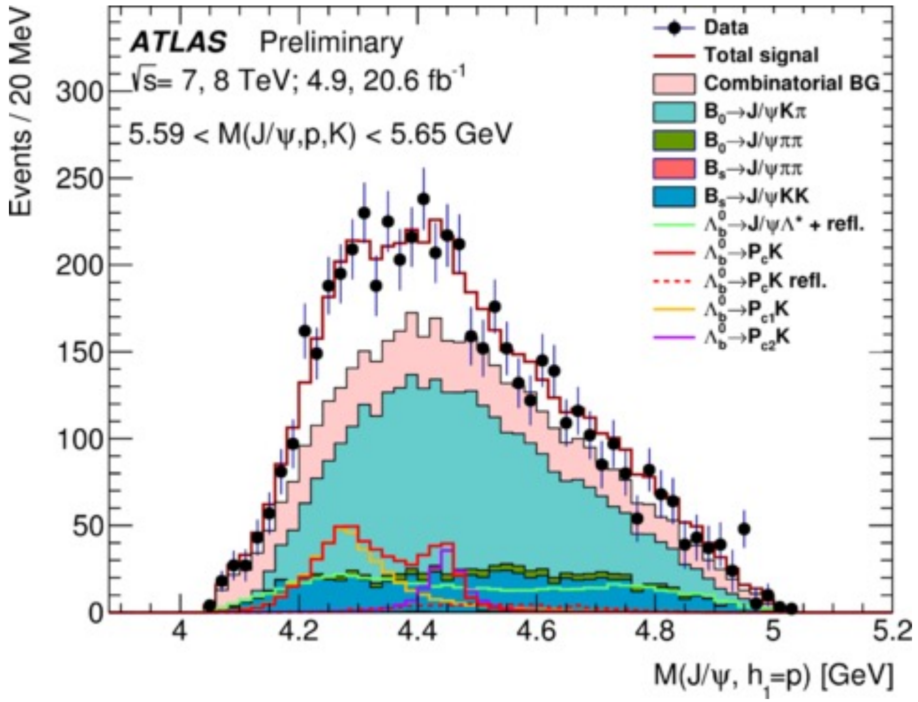

Hypothesis with two pentaquarks P_{c1} and P_{c2} with spin parity $3/2^-$ (lighter) and $5/2^+$ (heavier)

$P_c(4380)^+$ $P_c(4450)^+$

χ^2/N_{dof}=37.1/42

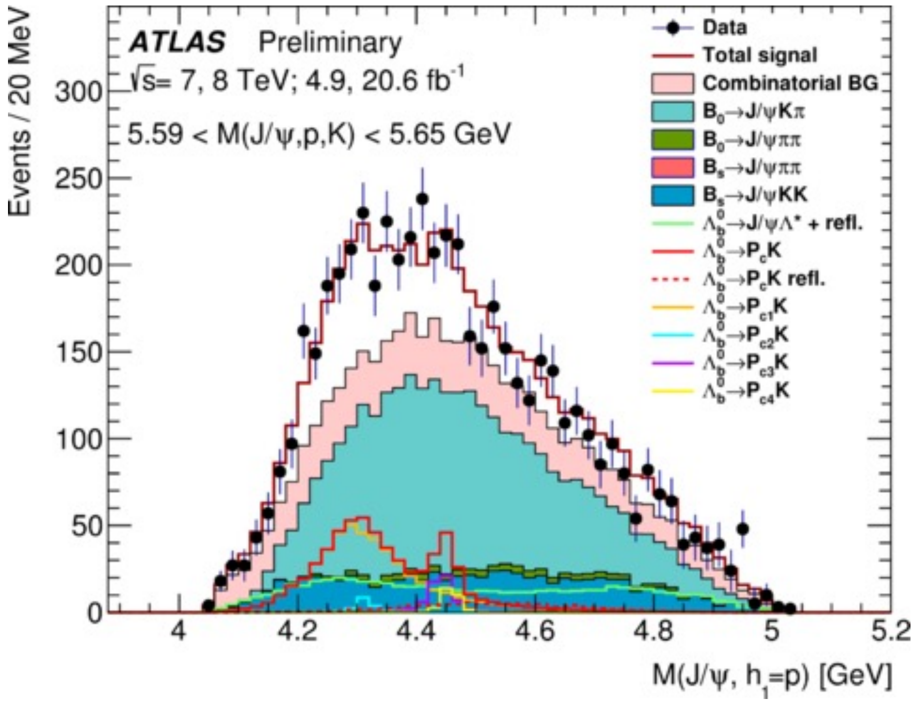

Hypothesis with four pentaquarks P_{c1},P_{c2},P_{c3},P_{c4}

Masses, widths, relative yields of narrow pentaquarks fixed to LHCb values

Pentaquarks in $\Lambda_b^0 \to J/\psi p K^-$

m(J/ψK)

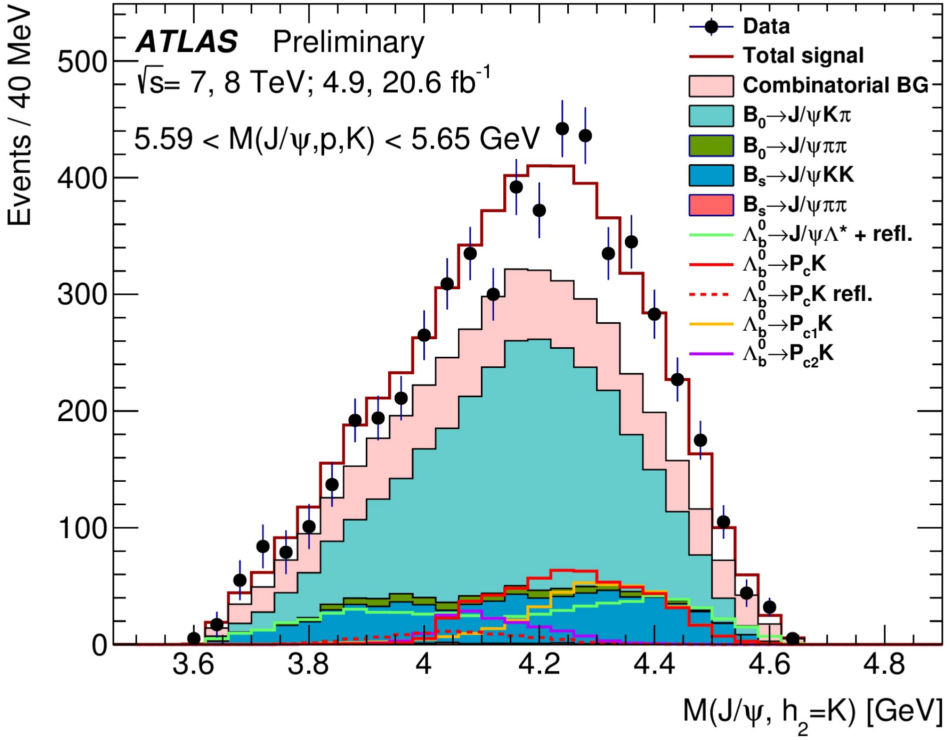

m(pK)

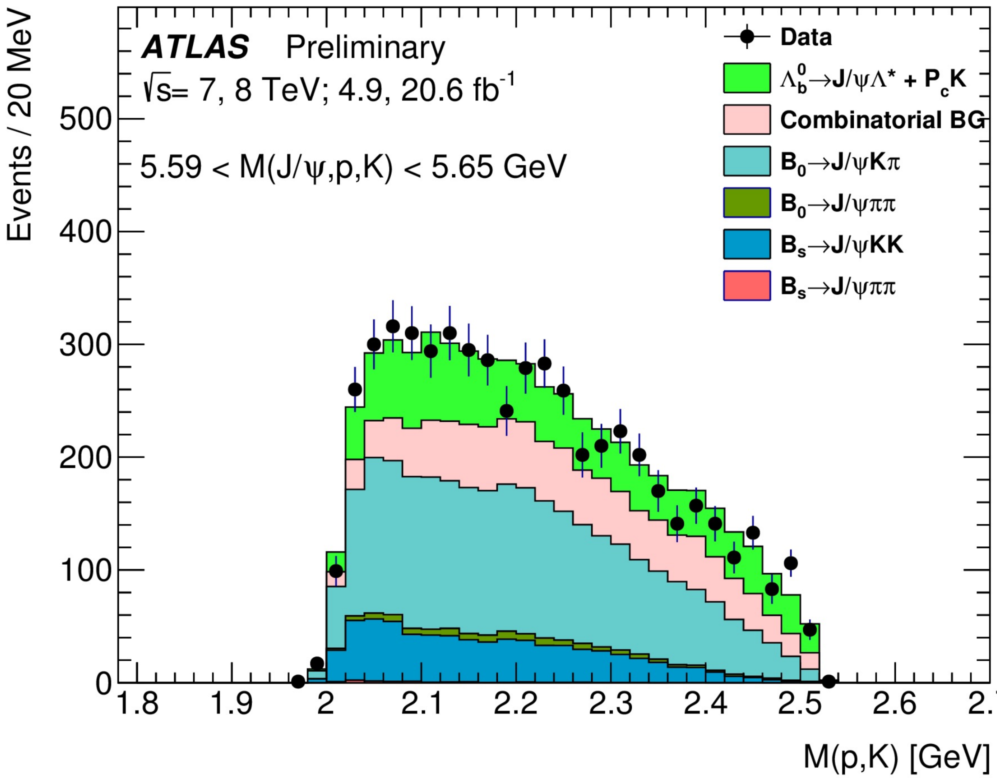

Projections of central fit results for two pentaquarks

Model with 2 pentaquarks describe the data well

Pentaquarks in $\Lambda_b^0 \to J/\psi p K^-$

Parameter	Value	LHCb value [5]
$N(P_{c1})$	$400^{+130}_{-140}(\text{stat})^{+110}_{-100}(\text{syst})$	–
$N(P_{c2})$	$150^{+170}_{-100}(\text{stat})^{+50}_{-90}(\text{syst})$	–
$N(P_{c1}+P_{c2})$	$540^{+80}_{-70}(\text{stat})^{+70}_{-80}(\text{syst})$	–
$\Delta\phi$	$2.8^{+1.0}_{-1.6}(\text{stat})^{+0.2}_{-0.1}(\text{syst})$ rad	–
$m(P_{c1})$	$4282^{+33}_{-26}(\text{stat})^{+28}_{-7}(\text{syst})$ MeV	$4380 \pm 8 \pm 29$ MeV
$\Gamma(P_{c1})$	140^{+77}_{-50} $(\text{stat})^{+41}_{-33}$ (syst) MeV	$205 \pm 18 \pm 86$ MeV
$m(P_{c2})$	4449^{+20}_{-29} $(\text{stat})^{+18}_{-10}$ (syst) MeV	$4449.8 \pm 1.7 \pm 2.5$ MeV
$\Gamma(P_{c2})$	51^{+59}_{-48} $(\text{stat})^{+14}_{-46}$ (syst) MeV	$39 \pm 5 \pm 19$ MeV

Masses and widths are all consistent with results from LHCb

Pentaquarks in $\Lambda_b^0 \rightarrow J/\psi p K^-$

- Analysis repeated without pentaquarks

- Descriptions of all distributions are not as good

- Data prefer model with two or more pentaquarks although model without pentaquarks cannot be excluded. χ^2 fit to m(J/ψ p) distribution gives p-value of 9.1 x 10^{-3}

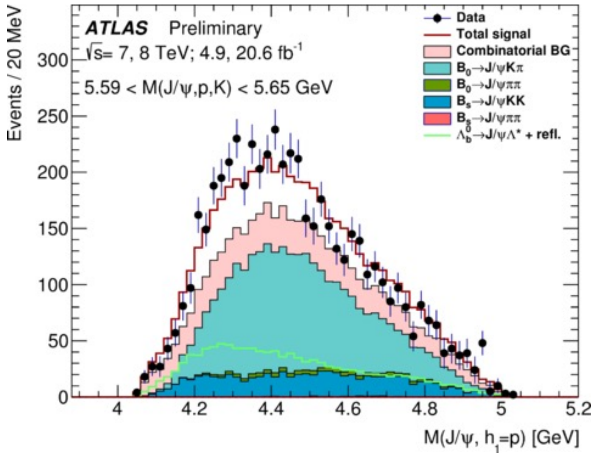

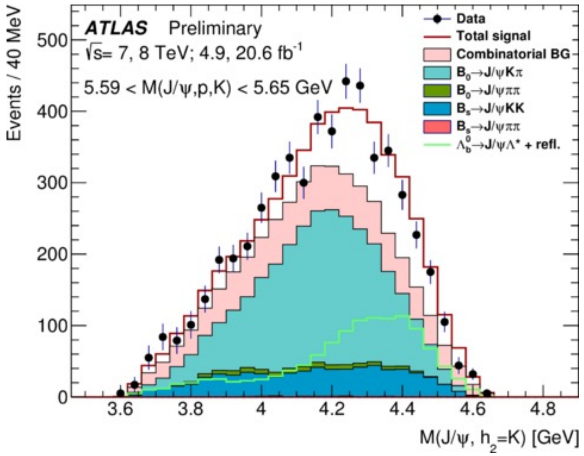

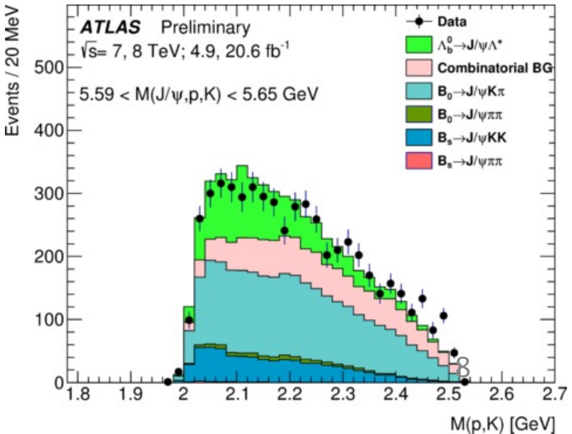

$B_c^+ \to J/\psi D_s^{(*)+}$

- $B_c^+ \to J/\psi D_s^{(*)+}$ can occur through b decay with c as spectator, or through annihilation diagram

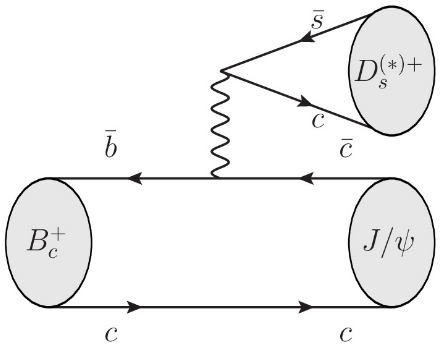

Color-favored spectator

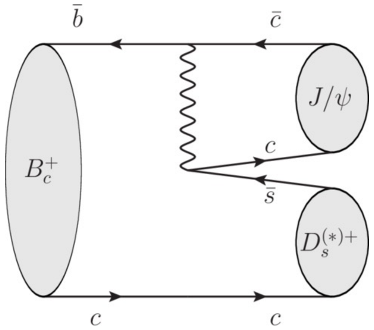

Color-suppressed spectator

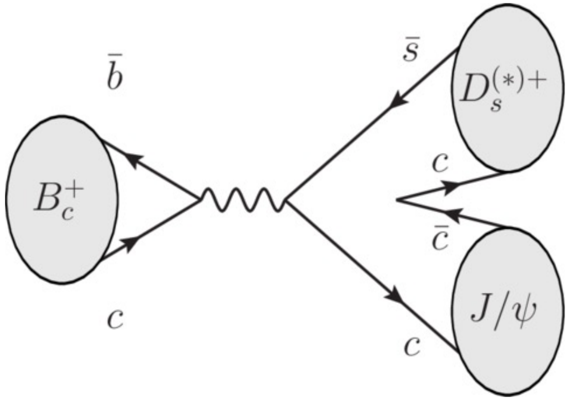

annihiliation

$B_c^+ \to J/\psi D_s^{(*)+}$ decays observed at LHCb (PRD 87 (2013) 112012) and ATLAS (EPJC 76 (2016) 4)

This analysis: Provide a more precise measurement of the $B_c^+ \to J/\psi D_s^{(*)+}$ branching fraction and polarization with full Run-2 data.

Useful for perturbative QCD calculations, relativistic potential models, sum rules calculations …

$B_c^+ \to J/\psi D_s^{(*)+}$

- $B_c^+ \to J/\psi(\mu^+\mu^-)D_s^+(\to \phi(\to K^+K^-)\pi^+)$
- $B_c^+ \to J/\psi(\mu^+\mu^-)D_s^{*+}(\to D_s^+\gamma/\pi^0)$ same reconstructed final state since soft neutral particle is not detected
- Reference channel for BR measurement: $B_c^+ \to J/\psi\pi^+$
- Fiducial range: $p_T(B_c^+) > 15$ GeV , $|\eta(B_c^+)| < 2.0$
- Measurements:
  - Ratio between BR of signal channels and $B_c^+ \to J/\psi\pi^+$: $R_{D_s^{(*)+}/\pi^+}$
  - Ratio between BR of signal channels to reduce uncertainties: $R_{D_s^{*+}/D_s^+}$
  - Transverse polarization fraction $\Gamma_{\pm\pm}/\Gamma$ for $B_c^+ \to J/\psi D_s^{*+}$

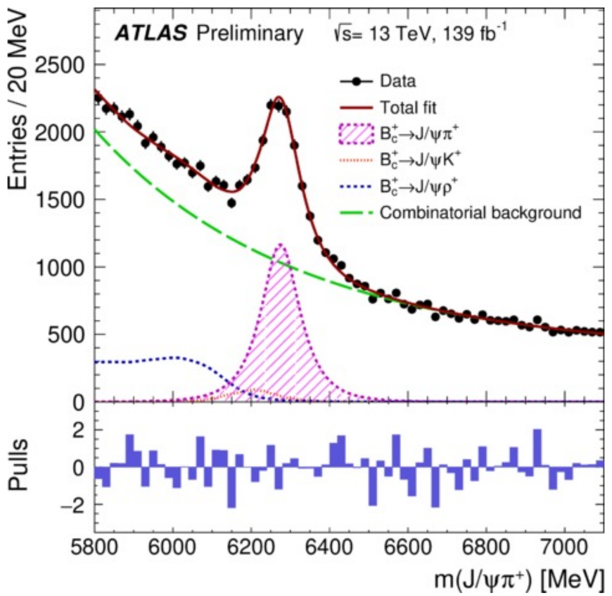

$B_c^+ \to J/\psi D_s^{(*)+}$

- Dataset 1: Candidates collected by standard dimuon or 3 muon triggers without requirements on additional inner detector track.
    - Can be used to measure $R_{D_s^+/\pi^+}$ and $R_{D_s^{*+}/\pi^+}$

- Dataset 2: Candidates collected only by dedicated $B_s^0 \to \mu^+\mu^-\phi$ triggers and not by other ones used in the analysis
    - Improve sensitivity to $R_{D_s^{*+}/D_s^+}$ and $\Gamma_{\pm\pm}/\Gamma$

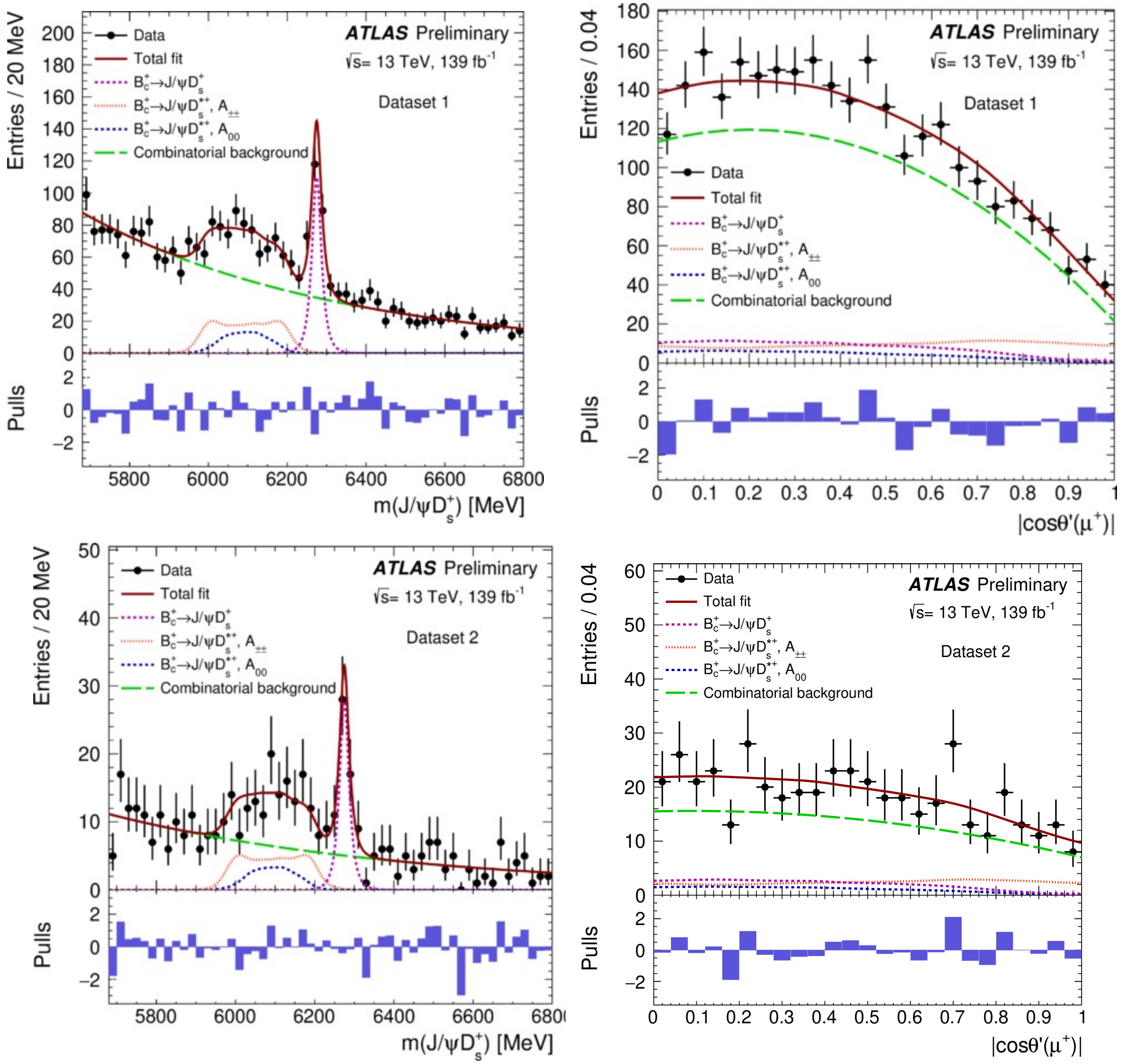

Results:

$R_{D_s^+/\pi^+}$ = 2.76 ± 0.33(stat.) ± 0.29(syst.) ± 0.16(br.f.)

$R_{D_s^{*+}/\pi^+}$ = 5.33 ± 0.61(stat.) ± 0.67(syst.) ± 0.32(br.f)

$R_{D_s^{*+}/D_s^+}$ = 1.93 ± 0.24(stat.) ± 0.10(syst.)

$\Gamma_{\pm\pm}/\Gamma$ = 0.70 ± 0.10(stat.) ± 0.04(syst.)

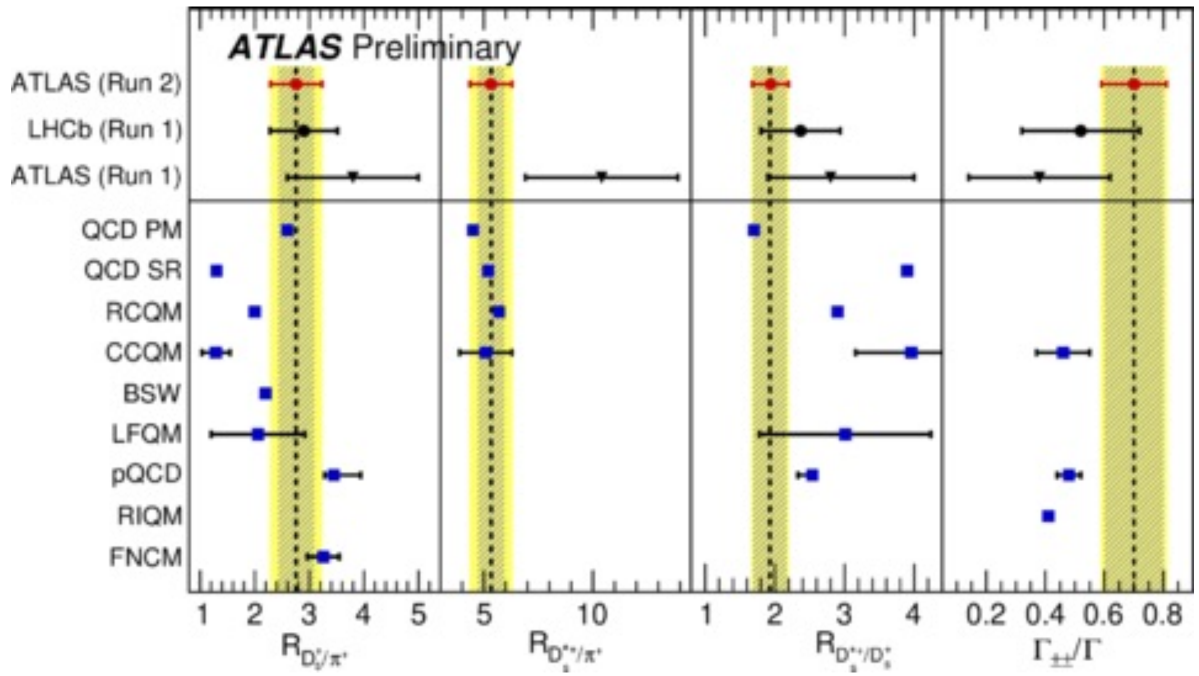

All results are consistent with the earlier measurements of ATLAS and LHCb

$R_{D_s^+/\pi^+}$	$R_{D_s^{*+}/\pi^+}$	$R_{D_s^{*+}/D_s^+}$	$\Gamma_{\pm\pm}/\Gamma$	Ref.
2.76 ± 0.47	5.33 ± 0.96	1.93 ± 0.26	0.70 ± 0.11	ATLAS Run 2
2.90 ± 0.62	–	2.37 ± 0.57	0.52 ± 0.20	LHCb Run 1 [1]
3.8 ± 1.2	10.4 ± 3.5	$2.8^{+1.2}_{-0.9}$	0.38 ± 0.24	ATLAS Run 1 [2]
2.6	4.5	1.7	–	QCD potential model [3]
1.3	5.2	3.9	–	QCD sum rules [4]
2.0	5.7	2.9	–	RCQM [5]
1.29 ± 0.26	5.09 ± 1.02	3.96 ± 0.80	0.46 ± 0.09	CCQM [6]
2.2	–	–	–	BSW [7]
2.06 ± 0.86	–	3.01 ± 1.23	–	LFQM [8]
$3.45^{+0.49}_{-0.17}$	–	$2.54^{+0.07}_{-0.21}$	0.48 ± 0.04	pQCD [9]
–	–	–	0.410	RIQM [10]
3.257 ± 0.293	–	–	–	FNCM [11]

The precision of the measurement exceeds that of all previous studies of these decays

QCD relativistic potential model describes well all three ratios

$X(5568)^{\pm}$ Search

ATLAS-CONF-2017-02. (PRL 120, 202007)

History:

Evidence from D0 of X(5568) state in
$X(5568)^{\pm} \rightarrow B_s\pi^{\pm}$ (PRL 117,022033,PRD 97,092004)

Not observed at:
CDF(PRL 120,202006)
LHCb(PRL 117,152003)
CMS (PRL,120,202005)

ATLAS Search using Run 1 data
$\sqrt{s}$=7 TeV, 4.9 fb^{-1}, $\sqrt{s}$= 8 TeV, 19.5 fb^{-1}

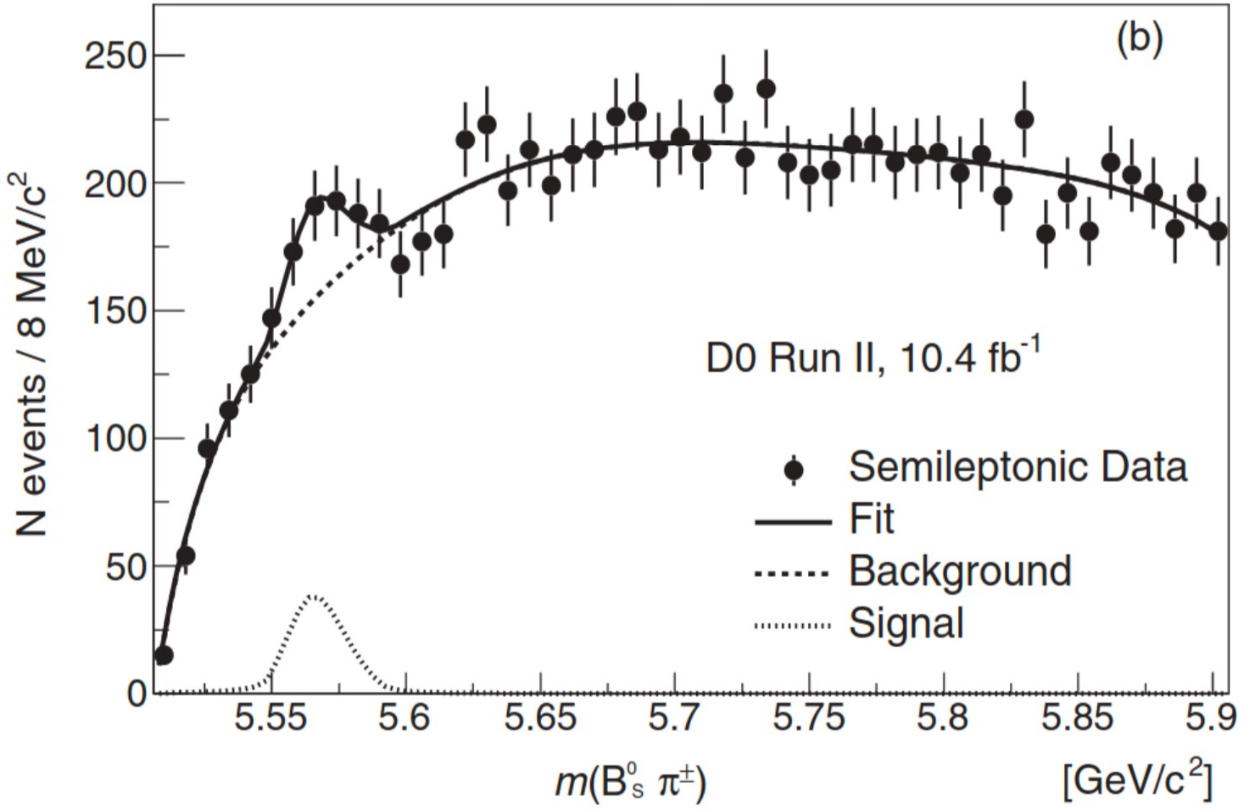

$X(5568)^{\pm}$ Search

B_s candidates

$p_T(\mu) > 4$ GeV, $p_T(K) > 1$GeV
Di-muon, di-kaon, and 4 track mass cuts
Di-muon and 4 track vertex cuts
$\tau(B_s) > 0.2$ ps

$B_s\ \pi$ reconstruction

$p_T(\pi) > 500$ MeV + primary vertex cut
$5346.6 < m(B_s) < 5386.6$ GeV

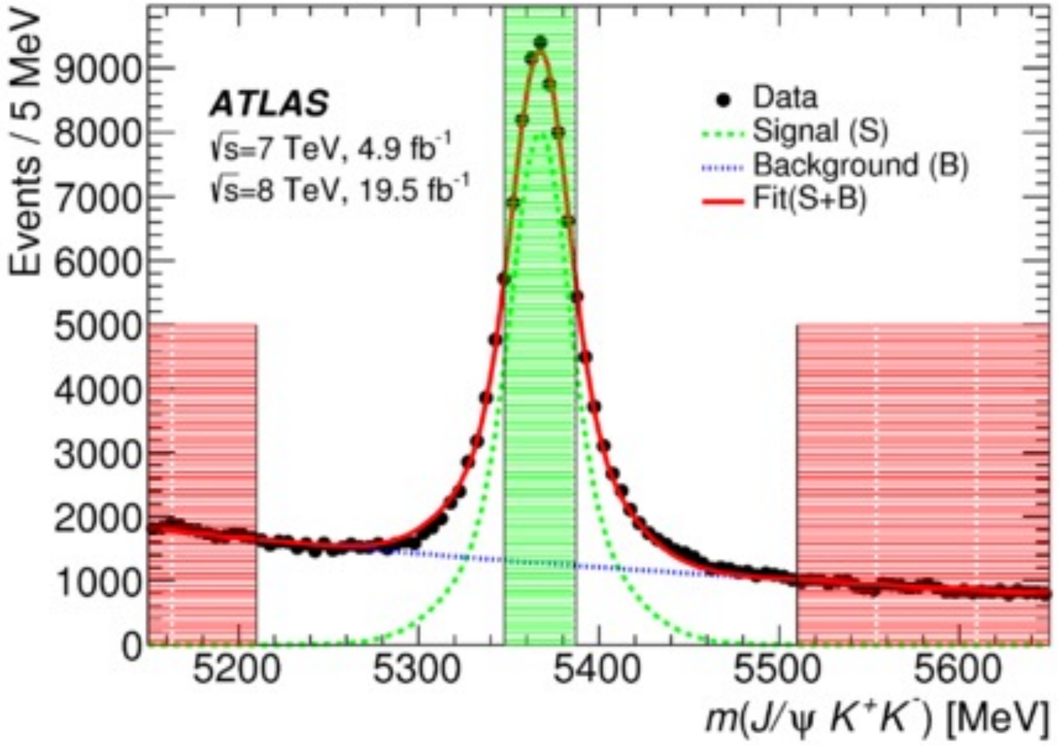

$X(5568)^{\pm}$ Search

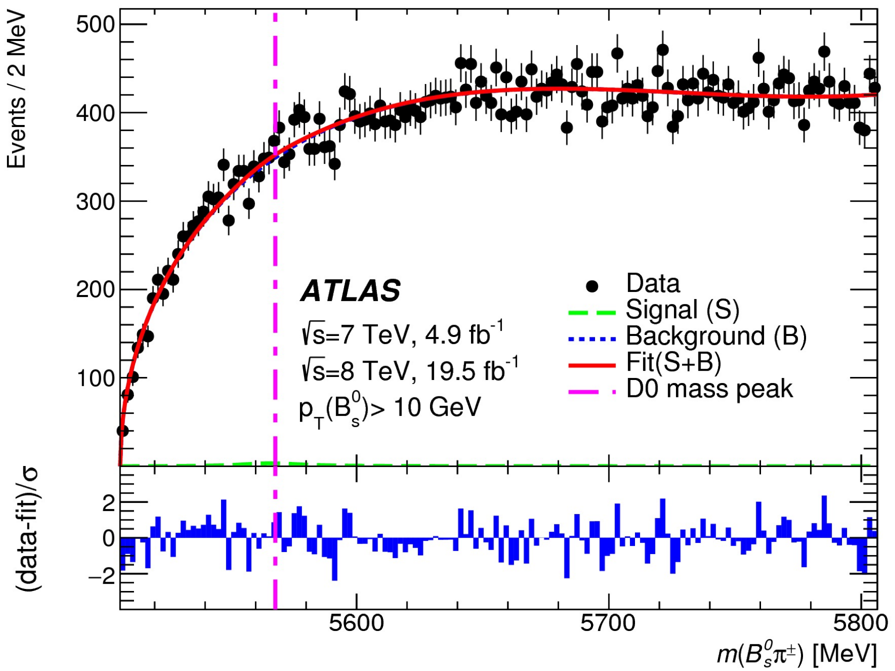

$p_T(B_s)$> 10 GeV

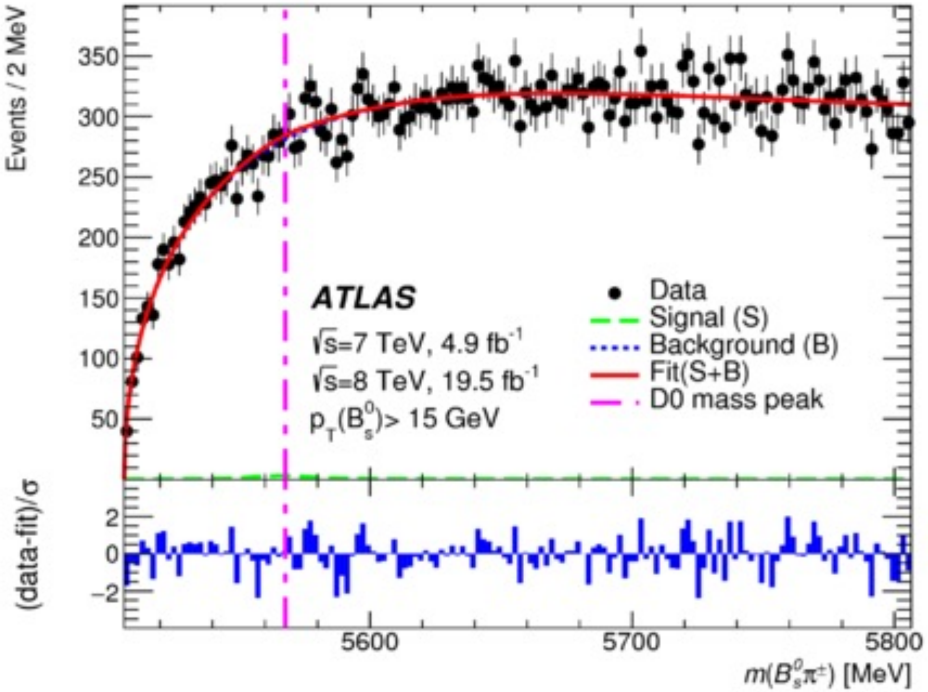

$p_T(B_s)$> 15 GeV

$X(5568)^{\pm}$ Search

- No evidence of a signal so set limits
- N_x: signal events and ρ_x: B_s fraction from $X(5568)^{\pm}$

$p_T(B_s)$> 10 GeV
N_x=60 $\pm$ 140
ρ_x< 1.5% at 95%CL

$p_T(B_s)$> 15 GeV
N_x=-30$\pm$150
ρ_x<1.6% @ 95% CL

Limits comparable to LHCb and CMS

No evidence of candidates at other masses in CLs scan

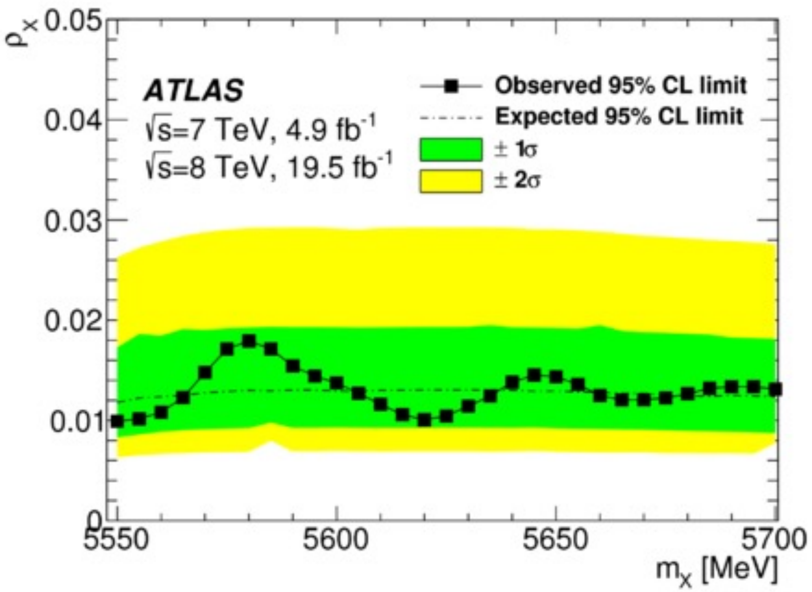

arXiv:1912.02672, Phys. Rev D 104, 012010

Relative B_c^+/B^+ production measurement at 8 TeV

- B_c^+ is the only known weakly decaying particle made up of two heavy quarks.
- Why study B_c^+ decays?
  - Test of QCD predictions
  - Input for heavy quark production models
  - Complements CMS/LHCb measurements
- Measurement of ratio: $\frac{\sigma(B_c^+)\cdot Br(B_c^+\to J/\psi\pi^+)\cdot Br(J/\psi\to\mu^+\mu^-)}{\sigma(B^+)\cdot Br(B^+\to J/\psi K^+)\cdot Br(J/\psi\to\mu^+\mu^-)}$
- Allows common systematics to nearly cancel.
- Measured in fiducial region $p_T(B)$> 13 GeV, |y(B)|<2.3
  - In addition 2 bins in P_T : 13<p_T(B) < 22 GeV and p_T(B) >22 GeV
  - 2 bins in rapidity |y(B)|< 0.75 and 0.75<|y(B)|<2.3)

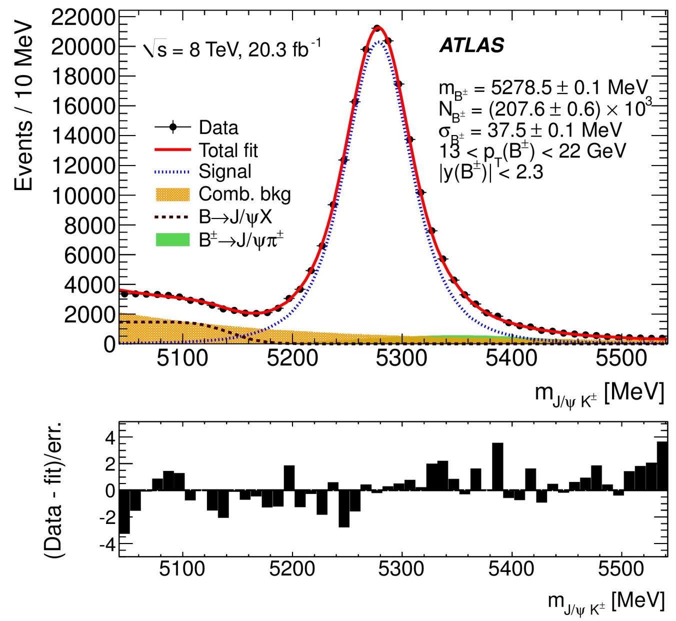

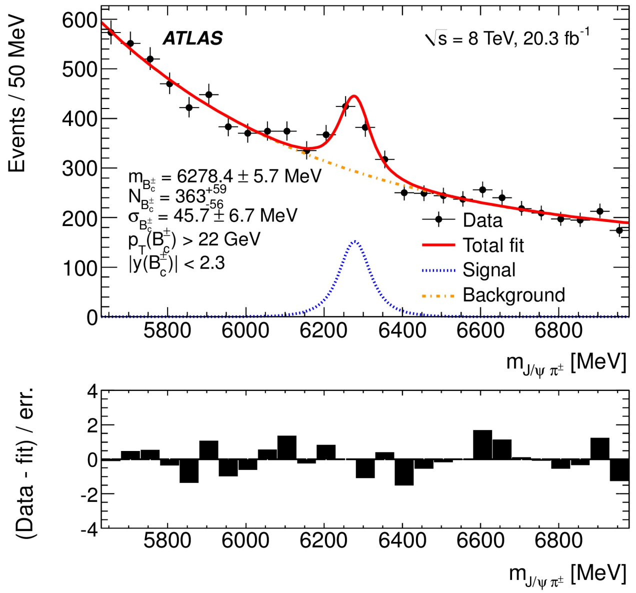

Results:

$$\frac{\sigma(B_c^+)\cdot Br(B_c^+\to J/\psi\pi^+)\cdot Br(J/\psi\to\mu^+\mu^-)}{\sigma(B^+)\cdot Br(B^+\to J/\psi K^+)\cdot Br(J/\psi\to\mu^+\mu^-)} =$$

$$(0.34 \pm 0.04(stat)^{+0.06}_{-0.02}(syst.) \pm 0.01(lifetime))\%$$

Production decreases faster with p_T for B_c than B^+

No evidence of any rapidity dependence

$0.683 \pm 0.018 \pm 0.009$	p_T<20 GeV, 2.0 <|y|< 4.5	LHCb 8 TeV
$0.48 \pm 0.05 \pm 0.03 \pm 0.05$	p_T>15 GeV, |y|<1.6.	CMS 7 TeV

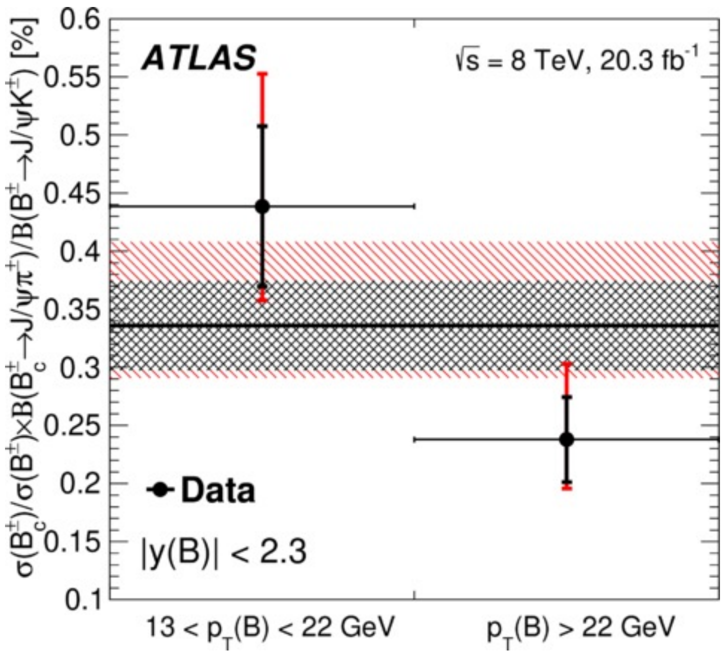

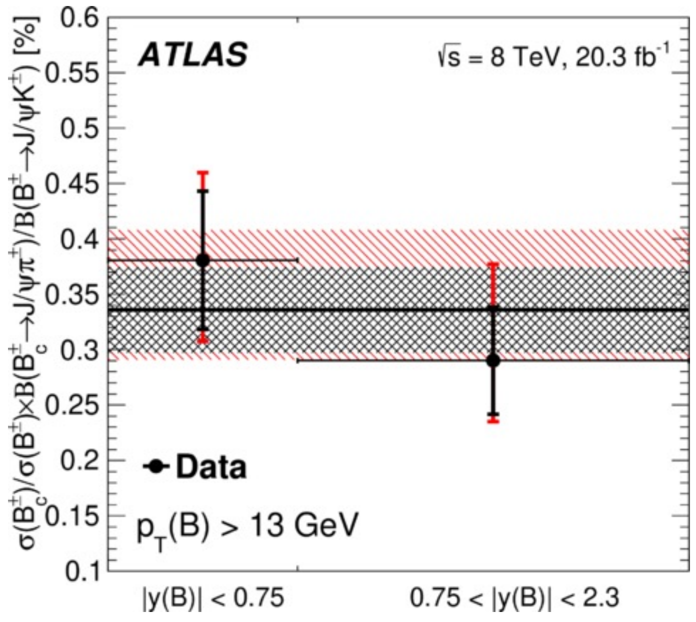

Analysis bin	$\sigma(B_c^\pm)/\sigma(B^\pm) \times \mathcal{B}(B_c^\pm \to J/\psi\pi^\pm)/\mathcal{B}(B^\pm \to J/\psi K^\pm)$
$p_T(B) > 13$ GeV, $\|y(B)\| < 2.3$	$(0.34 \pm 0.04_{\text{stat}}\,{}^{+0.06}_{-0.02\,\text{syst}} \pm 0.01_{\text{lifetime}})\%$
$13 < p_T(B) < 22$ GeV, $\|y(B)\| < 2.3$	$(0.44 \pm 0.07_{\text{stat}}\,{}^{+0.09}_{-0.04\,\text{syst}} \pm 0.01_{\text{lifetime}})\%$
$p_T(B) > 22$ GeV, $\|y(B)\| < 2.3$	$(0.24 \pm 0.04_{\text{stat}}\,{}^{+0.05}_{-0.01\,\text{syst}} \pm 0.01_{\text{lifetime}})\%$
$p_T(B) > 13$ GeV, $\|y(B)\| < 0.75$	$(0.38 \pm 0.06_{\text{stat}}\,{}^{+0.05}_{-0.04\,\text{syst}} \pm 0.01_{\text{lifetime}})\%$
$p_T(B) > 13$ GeV, $0.75 < \|y(B)\| < 2.3$	$(0.29 \pm 0.05_{\text{stat}}\,{}^{+0.07}_{-0.02\,\text{syst}} \pm 0.01_{\text{lifetime}})\%$

Conclusion:

- ATLAS has a rich heavy flavor physics program
- Many analyses statistically limited and will be updated with full Run2 dataset with improved detector performance
- Stay tuned for future results

Links

- (Pentaquark search). ATLAS-CONF-2019-048
- Study of the $B_c^+ \to J/\psi D_s^+$ and $B_c^+ \to J/\psi D_s^{*+}$ decays ATLAS-CONF-2021-046
- (X(5568) search) PRL 120, 202007 (2018)
- Relative B_c^+/B^+ production measurement at 8 TeV. Phys. Rev D 104, 012010 (2021)

Backup

$B_c^+ \to J/\psi\pi^+$ fit

Parameter	Value
$m_{B_c^+}$ [MeV]	6274.5 ± 1.5
$\sigma_{B_c^+}$ [MeV]	47.5 ± 2.5
$N_{B_c^+ \to J/\psi\pi^+}$	8440^{+550}_{-470}

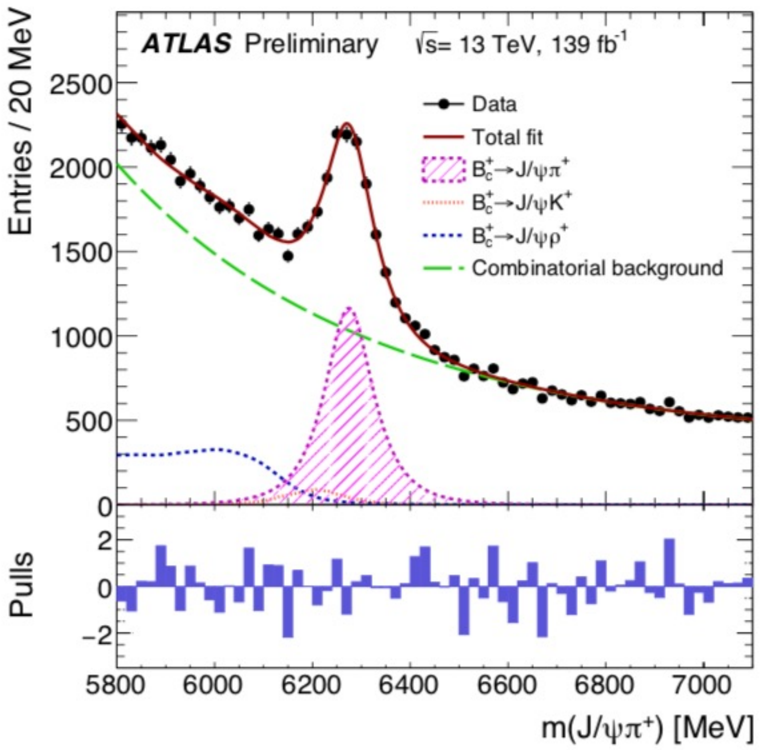

$B_c^+ \to J/\psi D_s^{(*)+}$ fit PDF

- 2D unbinned ML fit of $m(J/\psi D_s^+)$ and $|\cos\theta'(\mu^+)|$; mass and angular PDF are factorized
- ratio between $B_c^+ \to J/\psi D_s^+$ and $B_c^+ \to J/\psi D_s^{*+}$ yield and $f_{\pm\pm}$ are the same in DS1 and DS2
- $B_c^+ \to J/\psi D_s^+$ signal
  - *mass:* modified Gaussian[1]
  - *$|\cos\theta'(\mu^+)|$:* MC kernel template (same in DS1 and DS2)
- $B_c^+ \to J/\psi D_s^{*+}$ signals, separately $A_{\pm\pm}$ and A_{00} components
  - *mass:* MC kernel templates (same in DS1 and DS2)
  - *$|\cos\theta'(\mu^+)|$:* MC kernel templates (same in DS1 and DS2)
- Background
  - *mass:* exponential (same slope in DS1 and DS2)
  - *$|\cos\theta'(\mu^+)|$:* 2nd order polynomial (same parameters in DS1 and DS2)

[1] $Gauss^{mod} \propto \exp(-0.5 \times t^{1+1/(1+t/2)})$, where $t = |m(J/\psi D_s^+) - m_{B_c^+}|/\sigma_{B_c^+}$

$B_c^+ \to J/\psi D_s^{(*)+}$ fit result

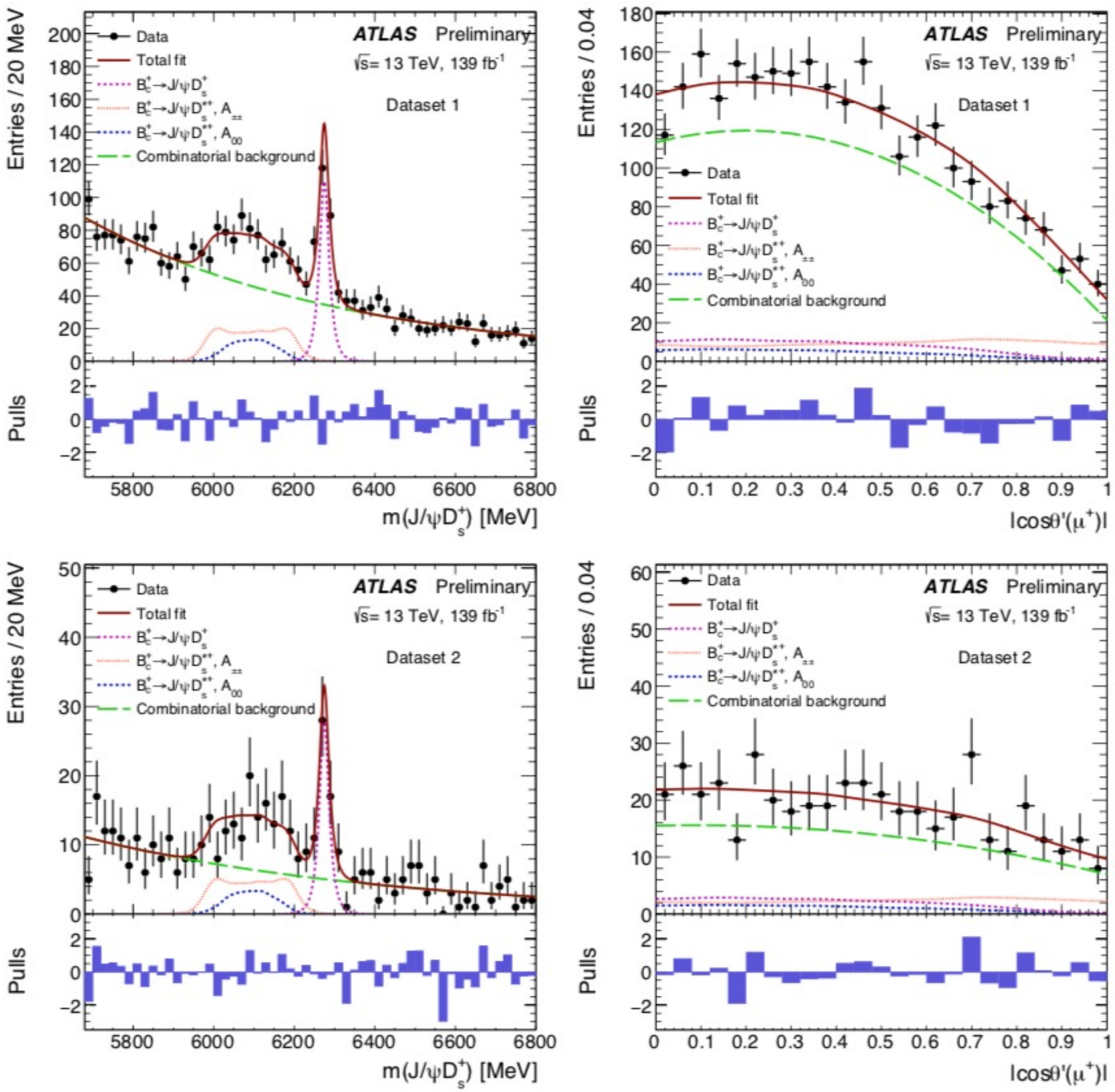

Parameter	Value
$m_{B_c^+}$ [MeV]	6274.8 ± 1.4
$\sigma_{B_c^+}$ [MeV]	11.5 ± 1.5
$r_{D_s^{*+}/D_s^+}$	1.76 ± 0.22
$f_{\pm\pm}$	0.70 ± 0.10
$N^{\text{DS1}}_{B_c^+ \to J/\psi D_s^+}$	193 ± 20
$N^{\text{DS2}}_{B_c^+ \to J/\psi D_s^+}$	49 ± 10
$N^{\text{DS1}}_{B_c^+ \to J/\psi D_s^{*+}}$	338 ± 32
$N^{\text{DS1\&2}}_{B_c^+ \to J/\psi D_s^+}$	241 ± 28
$N^{\text{DS1\&2}}_{B_c^+ \to J/\psi D_s^{*+}}$	424 ± 46

Ratios calculation

- $$R_{D_s^{(*)+}/\pi^+} = \frac{\mathcal{B}(B_c^+ \to J/\psi D_s^{(*)+})}{\mathcal{B}(B_c^+ \to J/\psi \pi^+)} = \frac{N^{\mathrm{DS1}}_{B_c^+ \to J/\psi D_s^{(*)+}}}{N_{B_c^+ \to J/\psi \pi^+}} \times \frac{\varepsilon_{B_c^+ \to J/\psi \pi^+}}{\varepsilon^{\mathrm{DS1}}_{B_c^+ \to J/\psi D_s^{(*)+}}} \times \frac{1}{\mathcal{B}(D_s^+ \to \phi(K^+K^-)\pi^+)}, \quad (1)$$
- $\mathcal{B}(D_s^+ \to \phi(K^+K^-)\pi^+)$ taken as $m(K^+K^-)$-dependent, using CLEO measurement, recalculated to $\pm 7\,\mathrm{MeV}$
- $$R_{D_s^{*+}/D_s^+} = \frac{\mathcal{B}(B_c^+ \to J/\psi D_s^{*+})}{\mathcal{B}(B_c^+ \to J/\psi D_s^+)} = \frac{N^{\mathrm{DS1\&2}}_{B_c^+ \to J/\psi D_s^{*+}}}{N^{\mathrm{DS1\&2}}_{B_c^+ \to J/\psi D_s^+}} \times \frac{\varepsilon^{\mathrm{DS1\&2}}_{B_c^+ \to J/\psi D_s^+}}{\varepsilon^{\mathrm{DS1\&2}}_{B_c^+ \to J/\psi D_s^{*+}}} = r_{D_s^{*+}/D_s^+} \times \frac{\varepsilon^{\mathrm{DS1\&2}}_{B_c^+ \to J/\psi D_s^+}}{\varepsilon^{\mathrm{DS1\&2}}_{B_c^+ \to J/\psi D_s^{*+}}}, \quad (2)$$
- $$\varepsilon_{B_c^+ \to J/\psi D_s^{*+}} = \frac{1}{f_{\pm\pm}/\varepsilon_{B_c^+ \to J/\psi D_s^{*+}, A_{\pm\pm}} + (1 - f_{\pm\pm})/\varepsilon_{B_c^+ \to J/\psi D_s^{*+}, A_{00}}}, \quad (3)$$
- $$\Gamma_{\pm\pm}/\Gamma = f_{\pm\pm} \times \frac{\varepsilon^{\mathrm{DS1\&2}}_{B_c^+ \to J/\psi D_s^{*+}}}{\varepsilon^{\mathrm{DS1\&2}}_{B_c^+ \to J/\psi D_s^{*+}, A_{\pm\pm}}}. \quad (4)$$

Mode	$\epsilon^{\mathrm{DS1}}_{B_c^+ \to J/\psi X}$ [%]	$\epsilon^{\mathrm{DS1\&2}}_{B_c^+ \to J/\psi X}$ [%]
$B_c^+ \to J/\psi D_s^+$	0.971 ± 0.012	1.163 ± 0.013
$B_c^+ \to J/\psi D_s^{*+}$, A_{00}	0.916 ± 0.012	1.088 ± 0.012
$B_c^+ \to J/\psi D_s^{*+}$, $A_{\pm\pm}$	0.868 ± 0.010	1.049 ± 0.011
$B_c^+ \to J/\psi \pi^+$	2.169 ± 0.018	–

$B_c^+ \to J/\psi D_s^{(*)+}$

Systematics

Source	Uncertainty [%]			
	$R_{D_s^+/\pi^+}$	$R_{D_s^{*+}/\pi^+}$	$R_{D_s^{*+}/D_s^+}$	$\Gamma_{\pm\pm}/\Gamma$
Simulated $p_T(B_c^+)$ spectrum	1.5	1.9	0.4	0.1
Simulated $\lvert\eta(B_c^+)\rvert$ spectrum	0.7	0.7	0.1	0.2
B_c^+ lifetime	0.1	< 0.1	–	–
D_s^+ lifetime	0.4	0.4	–	–
Tracking efficiency	1.0	1.0	< 0.1	< 0.1
Pile-up effects	1.0	1.0	–	–
χ^2/ndf cut efficiency	3.2	3.2	–	–
Impact parameter cuts efficiency	0.2	0.2	–	–
BDT cut efficiency	1.3	1.3	–	–
Trigger efficiency	1.0	1.0	–	–
$B_c^+ \to J/\psi D_s^{(*)+}$ signal fit:				
D_s^+ signal mass modelling	1.8	0.5	1.3	0.8
D_s^{*+} signal mass modelling	0.6	1.2	1.7	2.7
signal angular modelling	0.4	< 0.1	0.4	0.6
background mass modelling	6.0	9.0	3.2	1.0
background angular modelling	0.9	1.3	2.1	2.4
$B_s^0 \to \mu^+\mu^-\phi$ triggers	0.8	0.5	1.3	4.0
$B_c^+ \to J/\psi\pi^+$ signal fit				
signal modelling	4.2	4.2	–	–
PRD/comb. background modelling	5.8	5.8	–	–
CKM-suppr. background modelling	1.0	1.0	–	–
MC statistics	1.5	1.5	1.7	1.5
Total	10.7	12.6	5.0	5.8
$\mathcal{B}(D_s^+ \to \phi(K^+K^-)\pi^+)$	5.9	5.9	–	–

- Effect of muon reconstruction and identification efficiency uncertainty affects individual channel efficiencies by about 1–2%. However, for the measured quantities, due to cancellation in the efficiency ratios, it is found to be negligible.

Pentaquarks in $\Lambda_b^0 \to J/\psi p K^-$

Systematics

Source	$N(P_{c1})$	$N(P_{c2})$	$N(P_{c1}+P_{c2})$	$\Delta\phi$
Number of $\Lambda_b^0 \to J/\psi p K^-$ decays	$^{+1.8}_{-0.6}\%$	$^{+6.6}_{-9.2}\%$	$^{+1.6}_{-0.8}\%$	$^{+0.3}_{-0.0}\%$
Pentaquark modelling	$^{+21}_{-0}\%$	$^{+1}_{-22}\%$	$^{+8.7}_{-4.4}\%$	$^{+1.6}_{-0.0}\%$
Non-pentaquark $\Lambda_b^0 \to J/\psi p K^-$ modelling	$^{+14}_{-2}\%$	$^{+5}_{-44}\%$	$^{+9.2}_{-9.1}\%$	$^{+3.6}_{-1.6}\%$
Combinatorial background	$^{+0.7}_{-4.0}\%$	$^{+18}_{-5}\%$	$^{+4.2}_{-4.8}\%$	$^{+3.2}_{-0.0}\%$
B meson decays modelling	$^{+13}_{-25}\%$	$^{+28}_{-35}\%$	$^{+1.6}_{-9.3}\%$	$^{+0.5}_{-2.1}\%$
Total systematic uncertainty	$^{+28}_{-25}\%$	$^{+35}_{-61}\%$	$^{+14}_{-15}\%$	$^{+5.1}_{-2.7}\%$

Source	$m(P_{c1})$	$\Gamma(P_{c1})$	$m(P_{c2})$	$\Gamma(P_{c2})$
Number of $\Lambda_b^0 \to J/\psi p K^-$ decays	$^{+0.06}_{-0.03}\%$	$^{+3.5}_{-2.5}\%$	$^{+0.07}_{-0.04}\%$	$^{+7}_{-13}\%$
Pentaquark modelling	$^{+0.6}_{-0.0}\%$	$^{+18}_{-0}\%$	$^{+0.2}_{-0.0}\%$	$^{+0}_{-33}\%$
Non-pentaquark $\Lambda_b^0 \to J/\psi p K^-$ modelling	$^{+0.23}_{-0.05}\%$	$^{+9.2}_{-1.2}\%$	$^{+0.24}_{-0.02}\%$	$^{+2}_{-62}\%$
Combinatorial background	$^{+0.03}_{-0.15}\%$	$^{+0}_{-11}\%$	$^{+0.01}_{-0.17}\%$	$^{+22}_{-4}\%$
B meson decays modelling	$^{+0.24}_{-0.00}\%$	$^{+21}_{-21}\%$	$^{+0.27}_{-0.14}\%$	$^{+17}_{-57}\%$
Total systematic uncertainty	$^{+0.7}_{-0.2}\%$	$^{+30}_{-24}\%$	$^{+0.4}_{-0.2}\%$	$^{+28}_{-91}\%$

Relative B_c/B^+ production

Source of uncertainty	Uncertainty value			
	$B_c^{\pm}$		$B^{\pm}$	
	$13\,GeV < p_T < 22\,GeV$	$p_T > 22\,GeV$	$13\,GeV < p_T < 22\,GeV$	$p_T > 22\,GeV$
Signal model of the fit	2.4%	1.1%	0.1%	0.2%
CS and PRD components	$^{+19.3\%}_{-2.4\%}$	$^{+19.9\%}_{-2.4\%}$	0.5%	0.5%
Background model of the fit	1.7%	1.2%	0.2%	0.2%
Trigger and reconstruction effects	0.9%	0.8%	1.2%	1.2%
B-meson lifetime uncertainty	1.1%	0.9%	< 0.1%	< 0.1%

Source of uncertainty	Uncertainty value			
	$B_c^{\pm}$		$B^{\pm}$	
	$\|y\| < 0.75$	$0.75 < \|y\| < 2.3$	$\|y\| < 0.75$	$0.75 < \|y\| < 2.3$
Signal model of the fit	2.5%	2.8%	0.1%	0.2%
CS and PRD components	$^{+11.2\%}_{-2.4\%}$	$^{+23.2\%}_{-2.4\%}$	0.5%	0.5%
Background model of the fit	2.8%	1.3%	0.2%	0.2%
Trigger effects and reconstruction effects	1.1%	1.0%	1.2%	1.1%
B-meson lifetime uncertainty	1.0%	0.9%	< 0.1%	< 0.1%